

INSERTION OF HYDROGEN AND/OR LITHIUM INTO CESIUM TUNGSTEN BRONZE

Jana BLUDSKA¹, Jiri VONDRAK² and Ivo JAKUBEC³

Institute of Inorganic Chemistry, Academy of Sciences of the Czech Republic, 160 00 Prague 6, Czech Republic; e-mail: ¹ bludska@iic.cas.cz, ² vondrakj@iic.cas.cz, ³ jakubec@iic.cas.cz

Received February 26, 1997

Accepted June 2, 1997

Dedicated to Professor Jaromir Plesek on the occasion of his 70th birthday in recognition of his outstanding contribution to organic, borane and carborane chemistry.

Hydrogen and/or lithium insertion into hexagonal cesium tungsten bronze, $\text{Cs}_{0.3}\text{WO}_3$, was studied using voltammetric and a.c. admittance methods. The close values of stoichiometric coefficients for hydrogen and/or lithium in coinsertion bronzes as well as the close values of diffusion coefficients D_{H} and D_{Li} are ascribed to a lattice distortion caused by large cesium species which influence both equilibrium and the mobility of inserting species regardless of their different chemical nature.

Key words: Hydrogen insertion; Lithium insertion; Coinsertion tungsten bronzes.

Hexagonal tungsten bronzes, a class of compounds of general formula A_xWO_3 , where A is an electropositive metal, were reported by Magneli and Blomberg¹. Their hexagonal framework consists of layers of corner-sharing WO_6 octahedra and contains large hexagonal and smaller trigonal tunnels parallel to the [001] direction (Fig. 1). Guest species A, with exception for hydrogen and lithium, occupy only hexagonal tunnels, and the maximum molar fraction of those inserted species, x , in A_xWO_3 is 0.3. However, this limit, based on structural considerations, can be exceeded by insertion or coinsertion of hydrogen and/or lithium having ionic diameters so small that they can be placed in trigonal tunnels of the host material. In this way, the coinsertion compounds $\text{A}_x\text{Li}_y\text{WO}_3$ ($\text{A} = \text{K}, \text{Na}; x + y > 0.3$) were prepared²⁻⁴.

Kinetics of hydrogen insertion from gaseous phase into $\text{A}_{0.3}\text{WO}_3$ ($\text{A} = \text{K}, \text{NH}_4$ and Cs) was studied in our previous work⁵. It was found that the reaction rate of hydrogen sorption as well as the maximum molar fraction of hydrogen depend on the size of the guest species A.

This contribution deals with electrochemical insertion of hydrogen and/or lithium into hexagonal cesium tungsten bronze. The course of hydrogen insertion from aqueous solution will be compared with hydrogen insertion in the absence of water.

EXPERIMENTAL

Hexagonal cesium tungsten bronze was prepared by solid state reaction according to Magneli¹. The chemical composition of the polycrystalline product was checked by chemical analysis, and its hexagonal structure was verified by X-ray diffraction⁶. The diameter of particles, $2.5 \cdot 10^{-6}$ m, was determined by sedimentometry.

Electrodes were prepared from a mixture of polycrystalline material and PTFE (3 wt.%) which was pressed on platinum grids. The electrode area was 1 cm^2 .

The electrochemical behavior was studied in a three-electrode cell. Insertion of hydrogen was carried out in 1 M aqueous solution of HCl with a platinum sheet as the counter electrode and a saturated calomel electrode (SCE) as the reference electrode. Insertion of lithium was accomplished in non-aqueous electrolyte containing 1 M LiClO_4 in dry propylene carbonate (PC), with lithium rolls as both the reference and the counter electrodes. The content of water, checked by the Fischer titration, was below 20 ppm.

Potentiostat (PAR Model 263, EG&G) with lock-in amplifier controlled by computer was used to carry out electrochemical measurements. Cyclic voltammetry, potentiostatic chronoamperometry and a.c. admittance measurements were the main methods used. Hydrogen insertion was investigated in the potential range from 0.5 to -0.3 V vs SCE at a scan rate of 10 mV s^{-1} . Lithium insertion was studied in the potential range 2.0–3.5 V vs Li/Li^+ at a scan rate of 1 mV s^{-1} .

The impedance spectra were measured in 1 M LiClO_4/PC electrolyte within 2.24 and 2.56 V vs Li/Li^+ in 0.02 V steps. The spectra were generated over the frequency range $10 \text{ kHz} - 10^{-4} \text{ Hz}$ by superimposing a 5 mV amplitude of a.c. excitation on d.c. bias of potentiostat. At each potential a number of measured frequencies uniformly distributed across a log frequency decade was scanned from high to low values. The Boukamp program EQUIVCRT (EG&G software equipment) was used for identification of the components of impedance spectrum.

All experiments were conducted at room temperature.

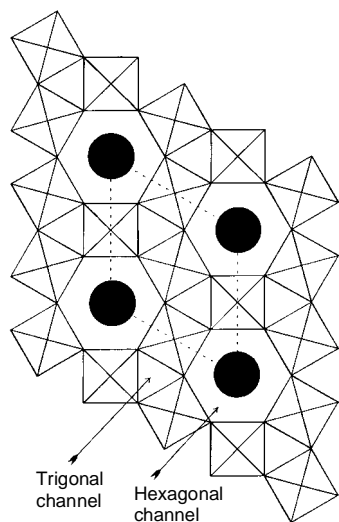


FIG. 1
Structure of hexagonal tungsten bronze, $\text{A}_{0.3}\text{WO}_3$
(A = K, Rb, Cs). Full circles: guest species A

RESULTS AND DISCUSSION

Hydrogen Insertion

Electrochemical insertion of hydrogen into hexagonal cesium tungsten bronze starts below 0.1 V vs SCE, as it is shown on the voltammetric curve in Fig. 2. The current increases with decreasing potential in the cathodic sweep giving two cathodic peaks at about 0.2 and -0.1 V vs SCE. Two peaks appear in the anodic sweep indicating expulsion of hydrogen from the host structure. During the subsequent cycling between 0.5 and -0.3 V vs SCE, the hysteresis was not observed and the system displayed an extraordinary good reversibility typical of WO_3 -based electrochromical systems.

From the voltammogram, potentials -0.1 and -0.3 V vs SCE were chosen for chronoamperometric measurements and $i-t$ curves were recorded to determine stoichiometric coefficients y and diffusion coefficients for hydrogen D_{H} in $\text{Cs}_{0.3}\text{H}_y\text{WO}_3$ at stated potentials.

An example of $i-t$ curve (measured at -0.3 V vs SCE) is shown in Fig. 3. The shape corresponds to a diffusion process restricted by the dimension of the available space (e.g., by the spherical shape of particles) according to the theory of diffusion processes⁷.

Constant potential -0.1 and -0.3 V vs SCE was applied on electrodes for a time necessary to reach steady-state current. The values of final background currents were then subtracted, the remainders were integrated and used for estimation of y in $\text{Cs}_{0.3}\text{H}_y\text{WO}_3$, 0.0002 and 0.0040, respectively.

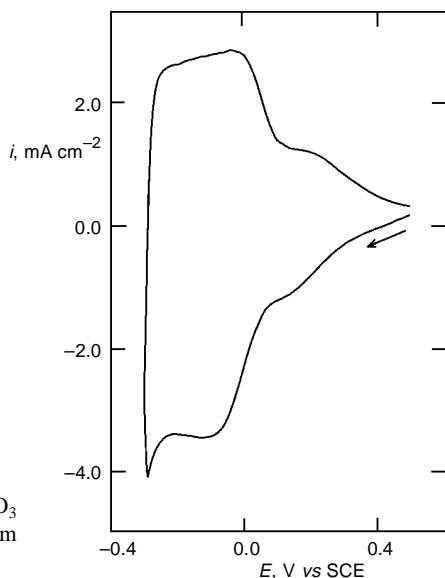


FIG. 2
Cyclic voltammogram of a hexagonal $\text{Cs}_{0.3}\text{WO}_3$ electrode in 1 M HCl. Scan rate 10 mV s^{-1} ; room temperature; surface area of electrode 1 cm^2

Further, the transient was plotted against $t^{-1/2}$, fitted by a linear equation in its intermediate part (see the inset in Fig. 3), and the Cottrell formula⁸,

$$i = F A \Delta y C_{H_0} (D_H / \pi t)^{1/2} + i_{\infty}, \quad (1)$$

was used for evaluation of diffusion coefficient. In this formula, i means current density, F is the Faraday constant, A is surface area, C_{H_0} is the concentration of available sites, Δy is the change in stoichiometric coefficient for hydrogen, t means time and i_{∞} is steady-state background current. Considering the density of tungsten trioxide, $\rho_{W O_3} = 7.0 \text{ g cm}^{-3}$ (ref.⁹), the density of cesium bronze, $\rho_{C s_{0.3} W O_3} = \rho_{W O_3} \cdot M_{C s_{0.3} W O_3} / M_{W O_3}$ equal to 8.2 g cm^{-3} , was calculated. Using this value of $\rho_{C s_{0.3} W O_3}$, the concentration of available sites, $C_{H_0} = 0.0301 \text{ mol cm}^{-3}$, and the surface area of spherical particles, $A = 3m / \rho_{C s_{0.3} W O_3} r$ (m is the mass of cesium bronze and r is the particle radius), were obtained. Then, diffusion coefficients $D_H = 1.6 \cdot 10^{-16}$ and $6.5 \cdot 10^{-18} \text{ m}^2 \text{ s}^{-1}$ were evaluated for hydrogen insertion at -0.1 and -0.3 V , respectively.

Hydrogen concentration in $C s_{0.3} H_y W O_3$, achieved after 1 h insertion at -0.3 V vs SCE in the aqueous electrolyte, $y = 0.004$, is the same as hydrogen concentration after 1 h hydrogen sorption from gaseous phase in the absence of water (see inset in Fig. 4). The value of diffusion coefficient D_H , $6.5 \cdot 10^{-18} \text{ m}^2 \text{ s}^{-1}$, obtained for hydrogen insertion at -0.3 V vs SCE , is in good agreement with the value of $8.5 \cdot 10^{-18} \text{ m}^2 \text{ s}^{-1}$, determined for hydrogen insertion in the absence of water⁵. However, a marked inhibition period appeared at the beginning of hydrogen sorption from gaseous phase (see inset in Fig. 4)

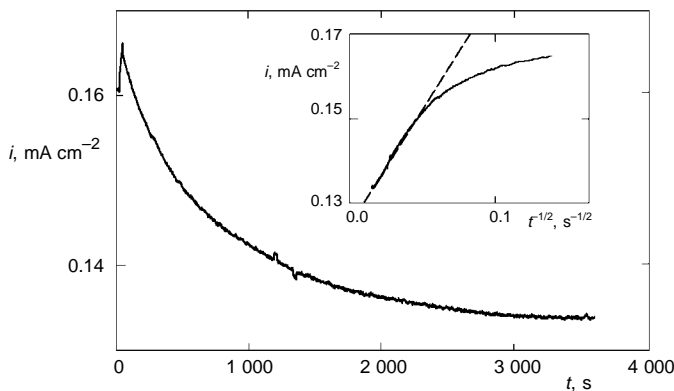


FIG. 3

Chronoamperometric curve of a hexagonal $C s_{0.3} W O_3$ electrode in 1 M HCl . Potential -0.3 V vs SCE ; room temperature; surface area of electrode: 1 cm^2 . Inset: Evaluation of the slope $F A \Delta y C_{H_0} (D_H / \pi)^{1/2}$ from the Cottrell equation (1)

which was not observed when traces of water were present in the reaction system¹⁰. We suppose that the accelerating role of water in hydrogen insertion consists in a facilitated transport of hydrogen particles along solvated chains which is faster than a simple translation motion.

Lithium Insertion

The electrochemical behavior of the hexagonal $\text{Cs}_{0.3}\text{WO}_3$ during insertion of lithium into this structure is displayed on the cyclic voltammograms in Fig. 5. The marked single wave, starting at about 2.8 V vs Li/Li⁺ in the cathodic sweep of the first voltammetric curve (1), indicates insertion of lithium. A single broad peak in the anodic sweep suggests the presence of a single insertion mechanism where lithium content is a function of potential. The shape of voltammetric curve is changed after 24 h anodic treatment of an electrode at 3.5 V vs Li/Li⁺. Then two broad peaks in the anodic sweep (Fig. 5, curve 2) indicate two kinds of insertion mechanism occurring in slightly different potential ranges. Taking into account partial extrication of cesium guests from hexagonal tunnels during the anodic delay, insertion of lithium species into both trigonal and hexagonal tunnels should be expected.

Lithium insertion into hexagonal cesium tungsten bronze was carried out under a constant potential of 2.4 V vs Li/Li⁺ which had been determined from the first voltammetric curve (see Fig. 5, curve 1). The value of stoichiometric coefficient in $\text{Cs}_{0.3}\text{Li}_y\text{WO}_3$, $y = 0.0036$, was estimated in the same way as in the case of hydrogen insertion. Then, the value of diffusion coefficient for lithium, $D_{\text{Li}} = 1.6 \cdot 10^{-17} \text{ m}^2 \text{ s}^{-1}$, was determined.

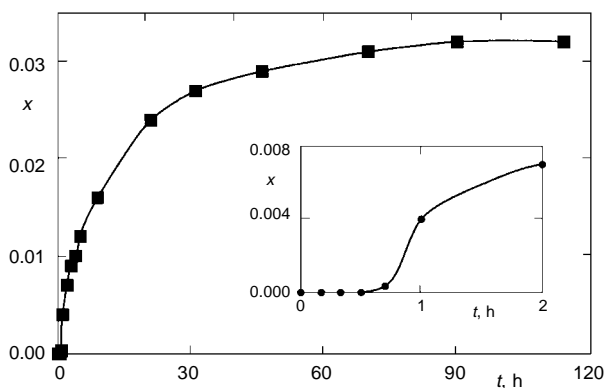


FIG. 4

Hydrogen insertion into hexagonal $\text{Cs}_{0.3}\text{WO}_3$ from gaseous phase in the absence of water. Hydrogen spill-over technique, 4 wt.% Pt : W; room temperature. Inset: Induction period at the beginning of sorption

Admittance Spectra

The electrode admittances were measured in the potential range close to 2.4 V where the insertion of lithium was expected according to voltammetric data. In Fig. 6, the entire series of admittance spectra is shown in a three-dimensional representation. Both the modulus of admittance on the vertical axis and the frequency on the horizontal axis are plotted in a logarithmic scale for all potentials. A low-frequency component with

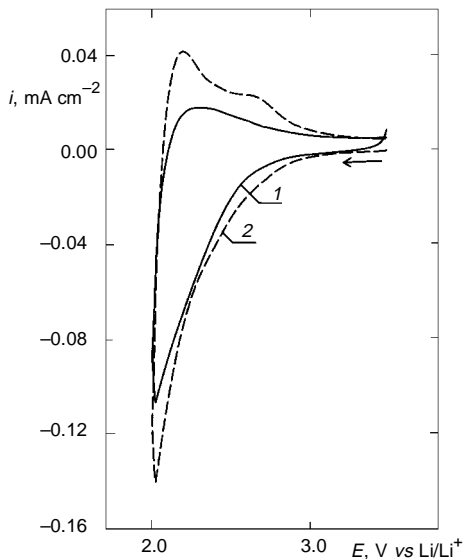


FIG. 5

Cyclic voltammograms of hexagonal $\text{Cs}_{0.3}\text{WO}_3$ electrode in 1 M LiClO_4 -propylene carbonate. Scan rate 1 mV s^{-1} ; room temperature; surface area of electrode 1 cm^2 . 1 First charge-discharge curve, 2 voltammetric curve measured after 24 h at 3.5 V vs Li/Li^+

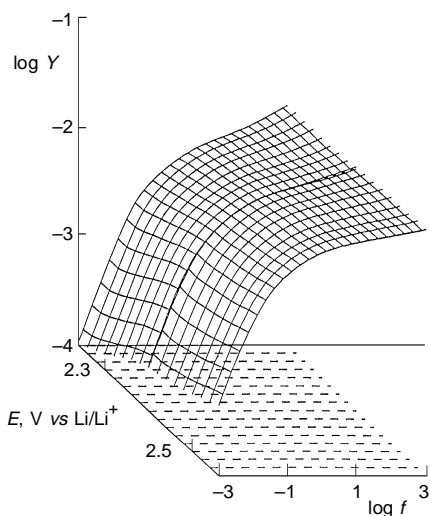


FIG. 6

Modulus of admittance Y (S) vs frequency f (Hz) in logarithmic scale. 1 M LiClO_4 -propylene carbonate; potential range 2.24–2.56 V vs Li/Li^+

the properties of a constant phase element (c.p.e.) is apparent as a small ridge in the vicinity of 2.4 V. This component of equivalent circuit is ascribed to the diffusion of lithium into the WO_3 matrix. Parallel to this element, double layer capacity and resistive component were found; they were almost independent of the electrode potential.

The values of constant phase elements of diffusional process, W , were obtained using the EQUIVCRT program and found to be proportional to a general power of frequency according to a relation $W = W_1 f^p$, where W_1 was a c.p.e. value extrapolated to frequency $f = 1$ Hz and an average experimental value of the exponent p was equal to 0.73. The c.p.e. values W_1 , plotted against potential, are shown in Fig. 7. This method allowed to improve the separation of the diffusion process from the background. In this way, the value $W_1 = 0.0036$ S over the background was found at frequency $f = 1$ Hz for potential of 2.4 V. Then, the value of diffusion coefficient $D_{\text{Li}} = 7.8 \cdot 10^{-18} \text{ m}^2 \text{ s}^{-1}$ was calculated, assuming the Randles–Grahame formula for diffusional admittance¹¹, which is in good agreement with the value D_{Li} obtained from potentiostatic measurements.

The values of stoichiometric coefficients of hydrogen and/or lithium in coininsertion cesium tungsten bronzes as well as the values of diffusion coefficients D_{H} and D_{Li} are fairly close. The rather low concentrations of inserted species can be ascribed to a lattice distortion of WO_3 matrix caused by large cesium species which affects both equilibrium and the mobility of inserting H and/or Li guests regardless of their different chemical nature.

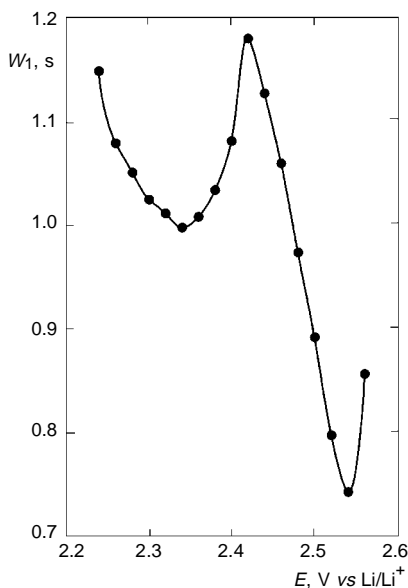


FIG. 7

Constant phase element of diffusional process W_1 vs potential. 1 M LiClO_4 -propylene carbonate; extrapolation for the frequency $f = 1$ Hz

The financial support of the Grant Agency of the Czech Republic (Grant No. 203/95/0101) is gratefully acknowledged.

REFERENCES

1. Magneli A., Blomberg B.: *Acta Chem. Scand.* 5, 372 (1951).
2. Banks E., Goldstein A.: *Inorg. Chem.* 7, 967 (1968).
3. Slade R. C. T., West B. C., Ramanan A., David W. I. F., Harrison T. A.: *Eur. J. Solid State Inorg. Chem.* 26, 15 (1989).
4. Slade R. C. T., West B. C., Hall G. P.: *Solid State Ionics* 32/33, 154 (1989).
5. Bludska J., Jakubec I.: *Z. Phys. Chem.* 196, 69 (1996).
6. Maixner J., Bezdicka P., Bludska J.: Unpublished results.
7. Crank J.: *The Mathematics of Diffusion*, 2nd ed., p. 89. Clarendon Press, Oxford 1995.
8. Bard A. J., Faulkner L. R.: *Electrochemical Methods*, p. 143. Wiley & Sons, New York, Chichester, Brisbane, Toronto 1980.
9. *CRC Handbook of Chemistry and Physics*, p. 4. CRC Press, Boca Raton, New York, London, Tokyo 1995.
10. Vondrak J., Bludska J.: *Solid State Ionics* 68, 317 (1994).
11. Bard A. J., Faulkner L. R.: *Ref.*⁸, p. 133.